

# Rogues' gallery: the full freedom of the Bianchi CMB anomalies

Andrew Pontzen\*

*Institute of Astronomy, Madingley Road, Cambridge CB3 0HA, UK*

(Dated: 14 January 2009)

Combining a recent derivation of the CMB evolution equations for homogeneous but anisotropic (Bianchi) cosmologies with an account of the full linearized dynamical freedoms available in such models, I calculate and discuss the various temperature and polarisation anisotropy patterns which may be formed. Certain anisotropies can be hidden in superhorizon modes at early times, thus avoiding any constraints from nucleosynthesis while nevertheless producing non-trivial redshift-zero temperature patterns in flat and open universes. The results are likely to be more of pedagogical than observational interest, but future work will assess whether such patterns can be matched to anomalies in WMAP results.

PACS numbers: 98.80.Es, 98.80.Jk

## I. INTRODUCTION

Bianchi universes – a large and almost complete class of relativistic models which are homogeneous but not necessarily isotropic – have remained of interest to mathematical cosmologists since seminal papers uncovering their major properties in the 1950s and 60s [e.g. 1, 2, 3, 4]; for a concise and accessible review see Ref. [5]. However for observers they are often considered obsolete, the chaotic cosmology programme having been superseded by the inflationary paradigm, especially in the light of CMB temperature maps from COBE [6] and WMAP [7] which are statistically very close to isotropy. On the other hand, there are deviations from the standard model predictions, consistent between COBE and WMAP, which are not easily linked to known systematics (e.g. [8, 9, 10] and references therein). Jaffe et al have shown [11] that anomalies such as the low quadrupole amplitude, alignment of low- $l$  modes and large-scale power asymmetry can be mimicked by adding (to the standard, scale-free perturbations which dominate the CMB signal) Bianchi temperature maps derived for a specific subclass of  $VII_h$  by Hawking and later Barrow [12, 13] (see also Ref. [14] in which the temperature patterns are discussed qualitatively by considering the Killing motions in a local orthonormal frame). Such models are more predictive than simple Bianchi I models which can trivially be fine-tuned to solve the quadrupole problem, e.g. [15, 16, 17]. Although the cosmological parameters implied by Jaffe et al's  $VII_h$  fit are inconsistent with concordance parameters [18, 19] and constraints from primordial nucleosynthesis [20], there is a possibility that these tensions may be resolved by a more complete dynamical model [18, 21, 22].

Recently, in Ref. [21] (henceforth PC07), a complete and computationally convenient Boltzmann hierarchy framework for calculating temperature and polarisation anisotropies in any nearly Friedmann-Robertson-Walker (FRW) Bianchi universe was described. For the

favoured parameters based on Jaffe et al's analysis of observed temperature maps, the predicted  $B$ -mode polarisation is too strong to be consistent with observational upper limits from WMAP three year data [23]. However, although the theoretical analysis was general, in numerical results PC07 followed previous Bianchi CMB studies in employing dynamical solutions for which the shear decays as  $\sigma \propto a^{-3}$ , where  $a$  is the FRW scale factor. It is as a direct result of this rapid decay that the polarisation amplitude is generally very strong relative to the anomalous temperature anisotropies; thus, like nucleosynthesis and density parameter inconsistencies, the polarisation conflict may be resolved by considering more general dynamics.

In this note, I discuss the appearance of the Bianchi CMB in the generalised nearly-isotropic regime. (Models which are highly anisotropic at any point after recombination are ruled out by observations if one assumes the Copernican principle [24].) I will show that the aforementioned polarisation and nucleosynthesis conflicts are simultaneously, yet naturally, avoided in a certain class of models. By fitting these models to CMB anomalies, constraints on cosmological parameters can be produced and tested against trusted concordance values; however, this requires a detailed statistical framework and is postponed to later work.

The setup and dynamics of the general case are described in §II and applied to flat and open models in §III. For pedagogical interest, I give results from models with a variety of cosmological parameters which are not necessarily consistent with other constraints. I describe the results for a closed universe in §IV although the anomalous CMB contribution in such cases is always a quadrupole and thus less interesting from a phenomenological standpoint. Finally, I summarise the work in §V.

## II. SET-UP AND DYNAMICS

During an epoch of near-isotropy, the dynamics of any Bianchi model can be analyzed by a decomposition into an isotropic FRW background and particular linear

---

\*Electronic address: apontzen@ast.cam.ac.uk

perturbations which break the isotropy while maintaining homogeneity with respect to three simply-transitive Killing vector fields (KVF's). For example, one might take an expanding flat model and perturb the expansion rates along one or two of the perpendicular coordinate axes; this canonical example arises as a special case (Type I) in the formalism described below.

The geometrical setup is described by the structure constants  $C_{ij}^k$  which fix the commutators of the three preferred Killing fields  $\vec{\xi}_i$ :

$$[\vec{\xi}_i, \vec{\xi}_j] = C_{ij}^k \vec{\xi}_k. \quad (1)$$

The explicit antisymmetry  $C_{ij}^k = -C_{ji}^k$  and the Jacobi identities  $C_{[bc}^a C_{e]a}^d = 0$  together substantially restrict the possible values for the  $C_{ij}^k$ ; in fact, up to arbitrary scalings and rotations only four of the initial 27 values are required to describe a given space (canonically [1] these are known as  $n_1, n_2, n_3$  and  $a_1$ , where  $a_1$  should be sharply distinguished from the FRW scale factor  $a$ ). The categorization of Bianchi models into distinct types rests on classifying the inequivalent sets of these four constants; here I will consider only the small subset which admit an FRW limit. Succinct but explicit derivations of the relations between structure constants and the resulting isotropic background cosmologies are available in PC07; or for more detail see e.g. Refs. [27, 29, 30].

I will first consider the open and flat models (Bianchi type VII<sub>h</sub> and its limiting types I, V and VII<sub>0</sub>); these possess two distinct geometric freedoms. The first corresponds to a characteristic length over which the Killing fields spiral relative to a parallel-propagated frame. In the canonical decomposition the physical scale of this spiral is fixed by setting  $n_1 = 0$ ,  $n_2 = n_3 = 1$  and scaling the present horizon size via the dimensionless Hubble parameter, usually denoted  $x$  [12, 31]. The second freedom corresponds to the isotropic curvature scale and can be set by specifying the fiducial FRW parameter  $\Omega_K$ , in terms of which  $a_1 = \pm x\sqrt{\Omega_K}$ . This sign ambiguity reflects a parity freedom; we will adopt the conventions of PC07 noting the standard result that, in terms of the CMB, parity inversion can be achieved by mirroring all maps and inverting the sign of  $B$  polarisation.

As  $x \rightarrow \infty$  for fixed  $\Omega_K$  one pushes spiral structure out of the horizon and obtains Type V models (this situation can be renormalized so that  $x = 1/\sqrt{\Omega_K}$ ,  $n_2 = n_3 = 0$  and  $a_1 = \pm 1$ ); for  $\Omega_K = 0$  we have the flat Type VII<sub>0</sub> specialisation ( $n_2 = n_3 = 1$ ,  $a_1 = 0$ ); with  $x \rightarrow \infty$  and  $\Omega_K = 0$  one obtains Type I (renormalisable such that  $x$  takes an arbitrary finite value with all structure constants vanishing), which was described at the start of this section.

Except in type I, the choice of canonical values preselects a preferred axis, rotations about which leave the structure constants invariant; the alignment of the perturbed shear eigenvectors relative to this axis determine both the patterns obtained in the CMB and the nature of the dynamics, but rotations around the axis are

pure gauge. Thus anisotropic perturbations are divided into three classes which transform respectively as scalars (henceforth  $s$ -modes), vectors ( $v$ -modes) and rank-2 tensors ( $t$ -modes) about the locally preferred axis; modes in these classes must evolve independently in the linear approximation [44]. The modes generate in turn  $m = 0, 1$  and 2 spherical harmonics in the CMB if the fiducial  $\theta = 0$  direction is taken along the residual symmetry axis (as in PC07). The general nearly-FRW Bianchi CMB appears as a linear combination of the three resulting patterns, although here we will study each mode separately.

A careful analysis of previous works [25, 26] shows that the linear amplitude  $A$  of any Bianchi mode evolves according to

$$A'' + 2\mathcal{H}A' + \lambda A = 0 \quad (2)$$

where primes denote the derivative with respect to conformal time  $\eta$ ,  $\mathcal{H} = a'/a$  is the conformal Hubble parameter,  $\lambda$  is a time-independent complex eigenvalue associated with each decoupled mode and the shear resulting from the mode has magnitude  $\sigma \propto |A'|/a$ . (When  $\lambda \notin \mathbb{R}$  the argument of the complex-valued  $A$  defines the orientation in the preferred plane; as previously stated the evolution equations are invariant under rotations in this plane,  $A \rightarrow Ae^{im\Delta\phi}$ .) Eq. (2) assumes there to be no anisotropic matter source terms, which in the absence of exotic effects should be a good approximation for the recombination era onwards (even if neutrino viscosity has an important role to play during radiation domination [e.g. 22, 28]).

Further technical discussion of the Bianchi linearisation and its relation to the existing literature will be given in a future work [27]; however, its essential features can be understood without the extensive framework required for a full derivation. For instance one may show that each mode maps onto a specific first order FRW metric perturbation (e.g. Bardeen [40]) with  $A$  proportional to the mode amplitude in the natural synchronous gauge defined by the Bianchi-homogeneous space slices. Seen from this perspective, the decaying modes correspond to vector perturbations (eq. 4.12 – 4.13 of Ref. [40], with Bardeen's  $\Psi \equiv A'$ ) and infinite wavelength gravitational waves (eq. 4.14 of Ref. [40], with  $k \rightarrow 0$  and Bardeen's  $H \equiv A$ ) whereas the oscillating modes correspond to gravitational waves of specific finite wavelengths (with our  $\lambda \equiv k^2 + 2K$ , where  $K$  is the FRW curvature parameter and  $k$  is the wavenumber in Ref. [40]). The particular wavelengths are associated, in the open and flat cases, with the aforementioned spiral lengthscale. Alternatively one may discern the physical status of the modes by considering gauge invariant covariant variables [30], in terms of which the oscillatory modes arise from the shear propagation equation ([30], eq. 31) as an interaction between shear and anisotropic 3-curvature ( $S \propto |\lambda A|/a^2$ ).

For closed (Type IX) models the canonical structure constants read  $n_1 = n_2 = n_3 = 1$ ,  $a_1 = 0$ ; in these units, the Hubble parameter is fixed by the FRW curvature

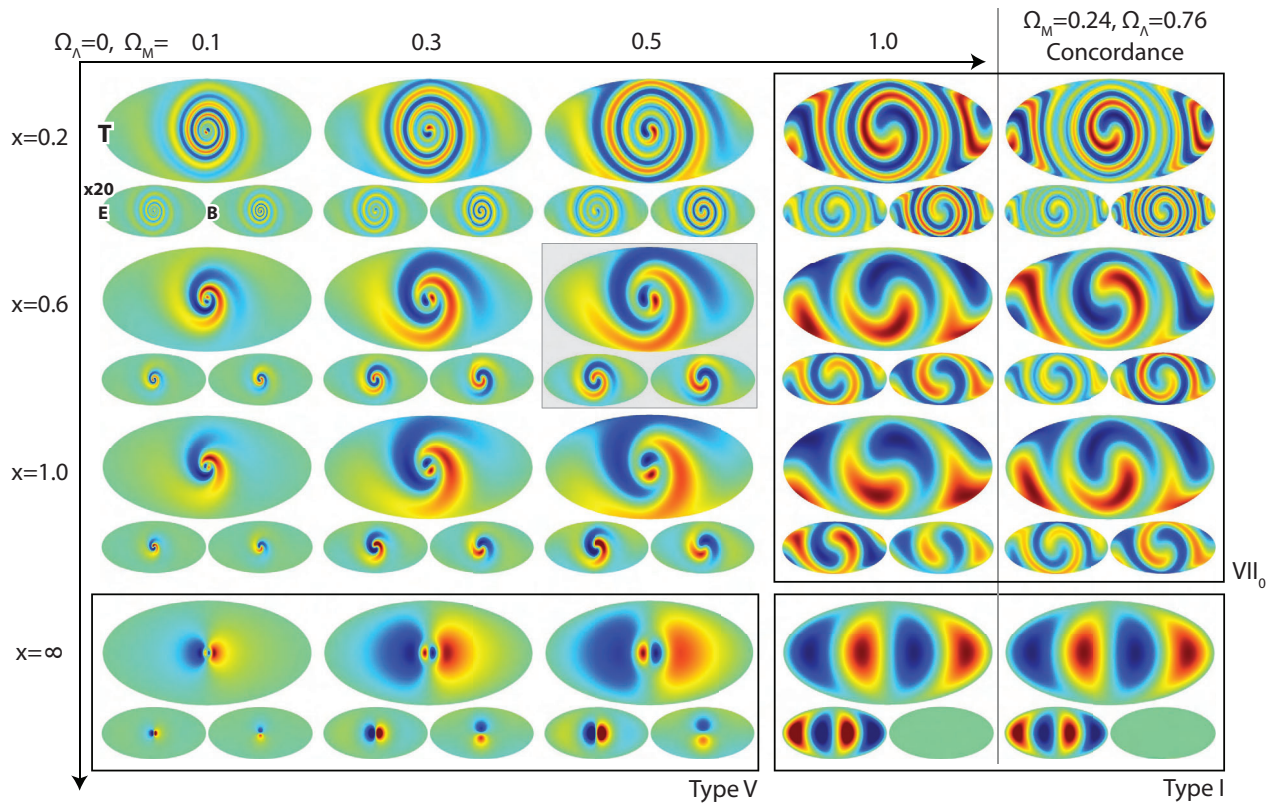


FIG. 1: The  $v$  (vector) modes of type  $VII_h$  and its specialisations. For a grid of parameters the temperature pattern is shown (upper panel) and  $E$  and  $B$  mode polarisation exaggerated in scale by a factor 20 (small lower left and right panels respectively).  $x$  varies from top to bottom while  $\Omega_M$  (and hence  $\Omega_K$ ) varies from left to right. I assume  $\Omega_\Lambda = 0$  except in the rightmost panels for which the concordance values ( $\Omega_M, \Omega_\Lambda = 0.24, 0.76$ ) are used. The primary effect of non-zero  $\Lambda$  is to increase the conformal time to last scattering, causing the final  $z = 0$  pattern to be more tightly wound. When  $\Omega_M + \Omega_\Lambda = 1$  one obtains type  $VII_0$ ; as  $x \rightarrow \infty$  one obtains type V (from  $VII_h$ ) or I (from  $VII_0$ ). The model with  $(\Omega_M, x) = (0.5, 0.6)$  (shaded panel) is able to mimic known CMB temperature anomalies [11, 19].

such that  $x = 1/\sqrt{-4\Omega_K}$ , i.e.  $K = 1/4$ . If the physical curvature radius is made progressively larger, we must take  $\Omega_K \rightarrow 0$  and  $x \rightarrow \infty$ . As before this limit yields, as expected, Type I models (explicitly by renormalizing such that  $n_1 = n_2 = n_3 = 0$  and  $x$  takes an arbitrary finite value). Further discussion of the closed models is deferred to §IV.

In all cases the physical value of  $H_0$  enters only through the recombination history which is obtained using RECFAST [32] assuming  $H_0 = 72 \text{ km s}^{-1} \text{ Mpc}^{-1}$  and  $\Omega_b = 0.044$ , but allowing  $\Omega_M$  and  $\Omega_\Lambda$  to vary consistently with the Bianchi model. For quantitative results in this pedagogic exploration I have ignored reionisation, discussing the effects of such an assumption individually for each mode.

### III. RESULTS: OPEN AND FLAT MODELS

In this section, I will discuss the possible patterns arising in the CMB when breaking the isotropy of open and flat FRW models; the relevant Bianchi type is  $VII_h$  (together with its previously described limiting cases). Of the three classes of linearized anisotropic freedoms discussed above it is the  $v$  modes [with  $\lambda = 0$  in Eq. (2)] which have been investigated in previous works on the Bianchi CMB [11, 18, 19, 21]; a grid of such models for varying  $x$  (vertical) and  $\Omega_M$  (horizontal) is shown in Fig. 1. A similar plot can be found in Ref. [33] but here I include the limiting types (V,  $VII_0$  and I) and additionally display the  $E$  and  $B$ -mode polarisation in two small panels beneath each temperature map. The model with  $(\Omega_M, x) = (0.5, 0.6)$  (shaded in Fig. 1) generates maps which mimic known CMB anomalies when suitably oriented on the sky [11, 19, 34]. The colour scale of the temperature plot is arbitrary (since one can rescale the linear perturbation to obtain any specified small mag-

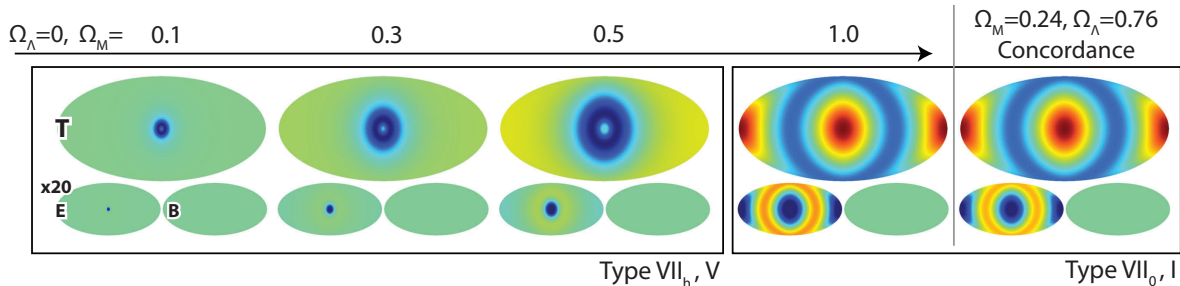


FIG. 2: The  $s$  (scalar) modes of all open and flat types are insensitive to the spiralling of the basis vectors, controlled by  $x$ , because the quadrupole anisotropy is aligned along the symmetry axis ( $m = 0$  in the decomposition of PC07). Similarly, no  $B$ -modes can be generated. In the  $VII_0/I$  limit, there is very little sensitivity to the value of  $\Omega_\Lambda$  since the anisotropy is always a pure quadrupole; only the relative polarisation strength is marginally affected (because of the increased conformal time to last scattering for larger  $\Omega_\Lambda$ ).

nitide) but the polarisation panels are shown exaggerated relative to the temperature panels by a factor of 20. Because the polarisation is already strong, reionisation would increase its strength only marginally (see PC07 for details).

While most models are calculated assuming  $\Lambda = 0$ , the final column displays concordance ( $\Omega_M, \Omega_\Lambda = 0.24, 0.76$ ) maps. The effect of non-zero  $\Lambda$  can be understood by examining equation (33) of PC07: the final patterns obtained are determined by  $a_1$  and the conformal time  $\eta$  to last scattering. Keeping these two quantities constant recovers the  $(\Omega_M, \Omega_\Lambda, x)$  degeneracy noted in previous works [18, 19] (although in the general case this picture is complicated somewhat by differing  $\sigma(a)$  behaviour when  $\lambda \neq 0$ ).

The  $VII_h s$  mode (Fig. 2) is similar to the  $v$  modes in its dynamical behaviour (also having curvature eigenvalue  $\lambda = 0$ ) and hence produces similar polarisation amplitudes. Because the mode is invariant under rotations about the preferred axis, the familiar spiral structure is missing (and hence the value of  $x$  has no effect). Further,  $B$ -mode polarisation is not generated (this is necessarily so when the transformation of the mode under reflections leaving the symmetry axis invariant is considered). The only remaining effect is the deformation of the quadrupole into a focussed spot, which cannot be evaded in anisotropic, homogeneous open universes [14, 27].

Of more interest are the  $VII_h t$  modes, which are dynamically non-trivial with curvature eigenvalue  $\lambda = 4(1 - ia_1)$  in Eq. (2). The resulting evolution is obtained numerically; however analytic approximations are helpful in interpreting the results. For instance during matter domination, while the isotropic curvature remains on superhorizon scales, we may assume  $\Omega_K = 0$  and  $\mathcal{H} = 2/\eta$ , yielding the explicit solution

$$A(\eta) = A_0 \left[ \frac{\cos 2\kappa\eta}{2(\kappa\eta)^3} + \frac{\sin 2\kappa\eta}{(\kappa\eta)^2} \right] + A_1 \left[ \frac{\sin 2\kappa\eta}{2(\kappa\eta)^3} - \frac{\cos 2\kappa\eta}{(\kappa\eta)^2} \right] \quad (3)$$

where the constant  $\kappa = \sqrt{\lambda}/2 = \sqrt{1 - ia_1}$  but physical results are unaffected by assuming  $\kappa \simeq 1$  [45].  $A_0$  and  $A_1$  are integration constants determined by boundary conditions, e.g. the shear and anisotropic curvature at a fixed time.

Modes with  $A_0 = 0, A_1 \neq 0$  ( $t_1$  modes) are regular as  $\eta \rightarrow 0$  (i.e. their dimensionless shear  $\sigma/H = |A'|/\mathcal{H}$  and anisotropic curvature  $S/H^2 = |\lambda A|/\mathcal{H}^2$  both tend to zero); conversely modes with  $A_0 \neq 0$  ( $t_0$  modes) have divergent anisotropy for  $\eta \rightarrow 0$ , thus predicting an early non-linear phase (which is not itself captured by our linear description). Although the picture is somewhat complicated by neutrino free-streaming, matching across matter-radiation equality shows that one may construct a  $t_1$  mode with small shear all the way to the initial singularity [46]. Thus by choosing a late-time solution with  $A_0 = 0$  one will automatically satisfy nucleosynthesis constraints (see also [35]). Furthermore, if the amplitude of all modes is set by some form of equipartition theorem at high redshifts (e.g. [28]), one may expect on entering the linear regime that the divergent  $t_0, v$  and  $s$  modes have similar amplitudes and decay rapidly to leave only these regular  $t_1$  modes. (However numerical models show that, with arbitrary initial conditions, the amplitude of the  $t_1$  mode is often sufficient to trigger a late-time non-linear anisotropic phase when it enters the horizon, e.g. [36], giving rise to the intermediate isotropisation picture in which homogeneous shear is only small for a finite period [43]. Of course if  $\Lambda \neq 0$ , this final non-linear phase can be avoided by shrinking the horizon again at late times.) One should bear in mind that  $t_0$  modes will generate similar CMB patterns but have radically different dynamical behaviour; however, I will not consider such a case quantitatively.

The patterns formed by the  $t_1$  mode are shown for a grid of parameters in Fig. 3. As  $x \rightarrow \infty$  the dimensionless curvature eigenvalue  $\lambda/x^2$  shrinks to zero (and thus the anisotropic curvature becomes pure gauge) – so no strict Type V or Type I limits exist for  $A_0 = 0$  and only

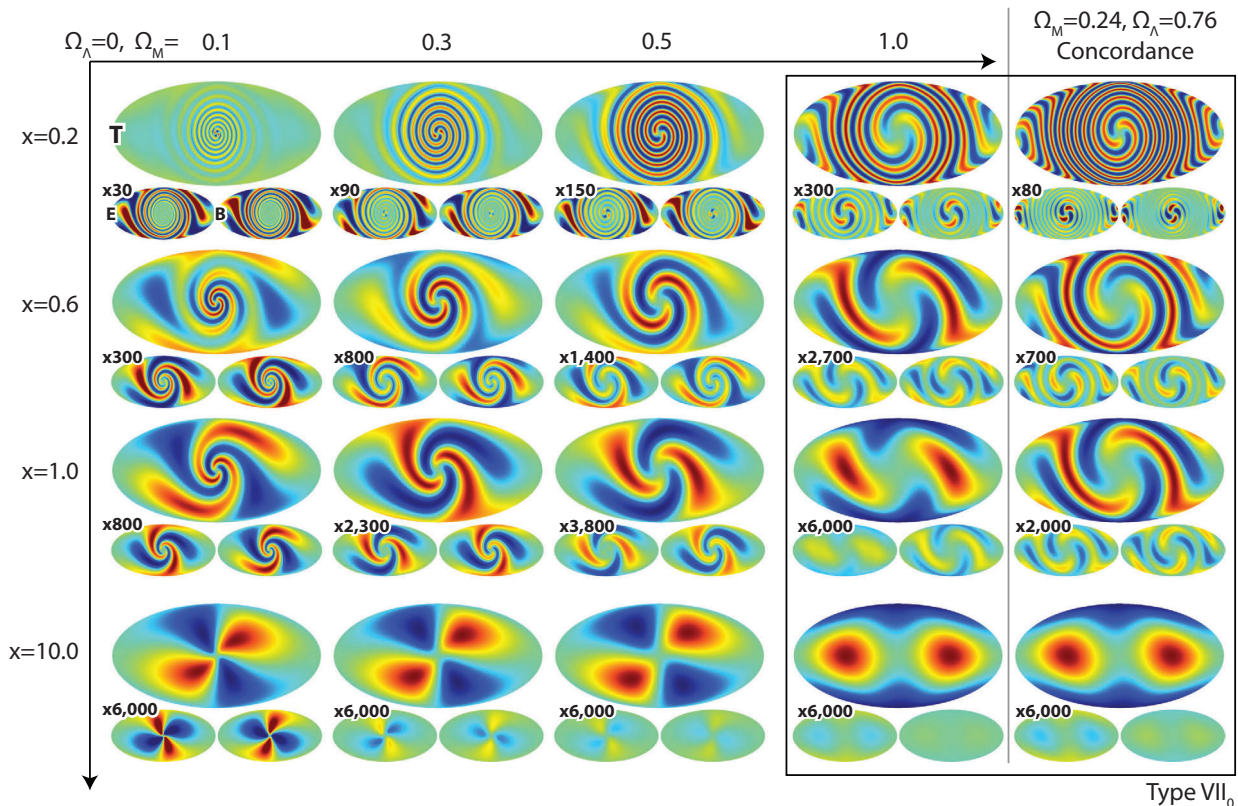


FIG. 3: The nucleosynthesis-compatible  $t_1$  modes of types  $VII_h$  and  $VII_0$ . The polarisation magnitude is exaggerated in scale by the factors specified in each subplot. The primary polarisation varies according to Eq. (7) and, because the shear can grow after recombination, is generally much weaker relative to the temperature anisotropy than with  $s$  and  $v$  modes for which the shear always decays.

finite values of  $x$  are considered. As before, the polarisation shown is purely primordial and ignores reionisation. The large variations in its strength between models can be understood by considering the shear near the decoupling surface. For models where  $\Omega_M$  is not tiny, effects are controlled by the long matter-dominated phase during which, unaware of small  $\Lambda$  or superhorizon isotropic curvature, observers see a flat Universe with effective Hubble parameter  $\sqrt{\Omega_M}x$ . For the polarisation strength one approximates

$$Q, U \propto \sigma_{\text{LSS}} \Delta t \propto \frac{A_1}{f_e x^2 \sqrt{\Omega_M} H_0 \Omega_b} \quad (4)$$

where  $\Delta t$  is the expected time between penultimate and final scattering,  $H_0$  is the physical Hubble parameter and  $f_e$  is the electron fraction at last scattering which scales approximately as  $\Omega_M^{1/2} \Omega_b^{-1} H_0^{-1}$  [e.g. 37]; since  $H_0$  and  $\Omega_b$  have been kept constant for all models, the overall polarisation anisotropy is taken to be proportional to  $A_1 x^{-2} \Omega_M^{-1}$ . On the other hand, the total temperature anisotropy is built up between  $z_{\text{LSS}} < z < 0$ . Ignoring the advection of the observed pattern to estimate the

magnitude of the temperature anisotropy we have

$$\Delta T \propto \int_{t_{\text{LSS}}}^{t_0} \sigma dt = \int_{\eta_{\text{LSS}}}^{\eta_0} A' d\eta = A(\eta_0) - A(\eta_{\text{LSS}}) \quad (5)$$

where  $\eta_0 = 2/(x\sqrt{\Omega_M})$  is the present day equivalent conformal time. Inserting the solution (3) one obtains the limits

$$\Delta T = A_1 \begin{cases} 8\eta_0^2/15 & \eta_0 \ll 1 \\ 4/3 & \eta_0 \gg 1. \end{cases} \quad (6)$$

The final polarisation-to-temperature ratio, combining Eqs (4) and (6), should scale roughly as

$$\frac{Q, U}{\Delta T} \propto \max\left(1, \frac{8}{5x^2 \Omega_M}\right) \quad (7)$$

which agrees with the trends shown in Fig. 3. Unlike the  $v$ ,  $s$  and  $t_0$  modes, here inclusion of reionisation will significantly boost the polarisation strength over the primordial expectation since the majority of models possess a considerably stronger temperature than polarisation quadrupole at  $z < 10$ .

An obvious question concerns the existence or otherwise of nucleosynthesis-compatible models which, in a

similar vein to the original VII<sub>h</sub>*v* fits (Fig. 1, shaded panel), can mimic known residual CMB anomalies. If this were possible using parameters consistent with concordance values, i.e. with maps from the right-hand column of Fig. 3, the type VII Bianchi models would command renewed observational interest. This will be investigated, comparing the maps developed here with data from WMAP [7], in future work.

#### IV. COMMENT: CLOSED MODELS

Type IX models have been shown by Grishchuk, Doroshkevich and Yudin [26] to decompose into a closed FRW background with superimposed maximal wavelength ( $k^2 = 6K$ ) gravitational wave perturbations (see also Ref. [38] for helpful comments) obeying the standard propagation equations ([40], eq. 4.14; see end of §II). Comparison shows that, within our terminology, this is modelled by the standard mode evolution (2) with  $\lambda = 2$  (this result is obtained directly from the anisotropic field equations in [27]).

By an extension of the arguments already presented, setting  $\kappa = \sqrt{2}$  in Eq. (3), one can see that the primary polarisation is again small for modes which evade nucleosynthesis constraints; however the temperature patterns are less phenomenologically interesting as they remain quadrupolar (at first order).

To see why this is, consider the origin of non-trivial patterns in the previously considered open and flat case. The temperature anisotropy  $\Delta T/T$  arises from integrating the shear tensor  $\sigma_{ij}$  projected, on each timeslice, along the tangent vector to the photon path (PC07, eq. 22). Taking the normalized spatial components  $p^i$  of the photon momentum (such that  $p^i p_i = 1$ ,  $i = 1 \dots 3$ ), one has

$$\frac{\Delta T(\theta_0, \phi_0)}{T} = - \int_{t_{\text{LSS}}}^{t_0} dt p^i(t; \theta_0, \phi_0) p^j(t; \theta_0, \phi_0) \sigma_{ij}(t) \quad (8)$$

where the integral is taken between last scattering ( $t_{\text{LSS}}$ ) and the time of observation ( $t_0$ ) and in general  $p^i$  is a function both of observation angles  $\theta_0, \phi_0$  and time  $t$ .

I have implicitly adopted a spatial chart such that all fluid quantities have constant components in a given spatial slice (this is always possible for Bianchi spaces; see PC07). In particular this means that the components of the shear tensor  $\sigma_{ij}$  depend only on time  $t$ , not on the observation angles. Written in this basis, non-quadrupolar temperature patterns can only arise through changes in the components of  $\vec{p}$  [at zeroth order for a first order solution to Eq. (8)]. In the Type IX case the components of  $p^i$  remain constant to this accuracy [47]; thus the temperature anisotropy remains purely quadrupolar.

According to the definitions in §II, the shear oscillates in time such that  $\sigma_{ij}(t) = a^{-1} A'(t) \tilde{\sigma}_{ij}$  for a fixed  $\tilde{\sigma}_{ij}$ . The temperature anisotropy (8) may be written  $\Delta T/T = (A(t_0) - A(t_{\text{LSS}})) \tilde{\sigma}_{ij} p^i p^j$  for the fixed observation vector  $\vec{p}(\theta_0, \phi_0)$ . Thus the quadrupole intensity

oscillates, the microwave background appearing exactly isotropic when  $A(t_0) = A(t_{\text{LSS}})$  which may occur an indefinite number of times depending on the initial conditions. Since  $x = 1/\sqrt{-4\Omega_K}$  (§II), the physical timescales over which the shear evolves are tied to the isotropic curvature lengthscale, consistent with the previously noted interpretation of Type IX anisotropies as maximal wavelength gravitational waves.

Although the temperature anisotropies remain quadrupolar,  $E$  and  $B$  modes mix; in fact PC07 eqs (33) or equivalently (50, 52) imply the polarisation type oscillates with period  $\Delta\eta = \pi$ . This effect can be traced to the need for the Killing fields to be everywhere non-vanishing and yet defined independently of the path followed between two points, leading to a spiralling of basis vectors perpendicular to a geodesic (see for example Fig. 1 in Ref. [38]).

Overall, type IX models can fit almost any combination of quadrupole anomalies in  $T$ ,  $E$  and  $B$  modes but, since no  $B$  modes can be generated while the universe remains optically thick, the ratio of the  $E$  to  $B$  anomalous quadrupole amplitudes determines (in the absence of reionisation) the conformal time to last scattering and hence constrains the FRW density parameters through the Hubble history. Reionisation complicates this picture, as does the existence of inhomogeneous modes superimposed on the FRW background, but in principle anomalous quadrupole moments are a powerful constraint for observers in closed anisotropic universes.

#### V. CONCLUSIONS

I have discussed anomalous CMB signals arising from broken FRW isotropy in open, flat and closed universes as described by mildly anisotropic Bianchi models. These are of interest both pedagogically and in the context of known CMB anomalies. It is possible to build anisotropic models which evade traditional constraints from nucleosynthesis by hiding the anisotropy in super-horizon gravitational waves which are pure gauge at early times. Whether such modes can be quantitatively linked to the observed CMB anomalies remains an open question which will be addressed in a future work.

It is important to stress that all effects discussed in this work, including for instance  $E$ - $B$  polarisation mixing, are purely gravitational and require no magnetic fields, extensions to general relativity or exotic matter source terms. Furthermore the models are predictive – polarisation-to-temperature ratios and (in the case of flat and open models) the detailed structure of the possible anomalous patterns are dictated by FRW density parameters which are constrained by a range of other observations. Thus a future Bianchi signal detection yielding consistent cosmological parameters, while highly surprising from the standpoint of present inflationary frameworks, would have to be taken seriously.

## Acknowledgments

I thank Anthony Challinor for collaboration on related work and many comments on the draft manuscript, Antony Lewis for helpful discussions, and the anonymous referee for suggestions which improved the presentation. Financial support is acknowledged from an STFC studentship and scholarship at St John's College, Cambridge.

- 
- [1] G. Ellis and M. MacCallum, *Commun. Math. Phys.* **12**, 108 (1969).
- [2] F. Estabrook, H. Wahlquist, and C. Behr, *J. Math. Phys.* **9**, 497 (1968).
- [3] O. Heckmann and E. Schucking, in *Gravitation: An Introduction to Current Research* (Wiley, New York, 1962), Chap. 11, p. 438.
- [4] A. Taub, *Ann. Math.* **53**, 472 (1951).
- [5] G. F. R. Ellis, *Gen. Relativ. Gravit.* **38**, 1003 (2006).
- [6] G. F. Smoot *et al.*, *Astrophys. J. Lett.* **396**, L1 (1992).
- [7] G. Hinshaw *et al.*, *Astrophys. J. Suppl. Ser.* (to be published), arXiv:0803.0732 (2008).
- [8] K. Land and J. Magueijo, *Phys. Rev. Lett.* **95**, 071301 (2005).
- [9] A. de Oliveira-Costa and M. Tegmark, *Phys. Rev. D* **74**, 023005 (2006).
- [10] C. J. Copi, D. Huterer, D. J. Schwarz, and G. D. Starkman, *Phys. Rev. D* **75**, 023507 (2007).
- [11] T. R. Jaffe *et al.*, *Astrophys. J. Lett.* **629**, L1 (2005).
- [12] C. B. Collins and S. W. Hawking, *Mon. Not. R. Astron. Soc.* **162**, 307 (1973).
- [13] J. D. Barrow, R. Juszkiewicz, and D. H. Sonoda, *Mon. Not. R. Astron. Soc.* **213**, 917 (1985).
- [14] J. D. Barrow and J. Levin, *Physics Letters A* **233**, 169 (1997).
- [15] L. Campanelli, P. Cea, and L. Tedesco, *Phys. Rev. Lett.* **97**, 131302 (2006).
- [16] D. C. Rodrigues, *Phys. Rev. D* **77**, 023534 (2008).
- [17] T. Koivisto and D. F. Mota, *Astrophys. J.* **679**, 1 (2008).
- [18] T. R. Jaffe, S. Hervik, A. J. Banday, and K. M. Górski, *Astrophys. J.* **644**, 701 (2006).
- [19] M. Bridges, J. D. McEwen, A. N. Lasenby, and M. P. Hobson, *Mon. Not. R. Astron. Soc.* **377**, 1473 (2007).
- [20] J. Barrow, *Mon. Not. R. Astron. Soc.* **175**, 359 (1976).
- [21] A. Pontzen and A. Challinor, *Mon. Not. R. Astron. Soc.* **380**, 1387 (2007).
- [22] J. D. Barrow, *Phys. Rev. D* **55**, 7451 (1997).
- [23] L. Page *et al.*, *Astrophys. J. Suppl. Ser.* **170**, 335 (2007).
- [24] W. R. Stoeger, R. Maartens, and G. F. R. Ellis, *Astrophys. J.* **443**, 1 (1995).
- [25] C. B. Collins and S. W. Hawking, *Astrophys. J.* **180**, 317 (1973).
- [26] L. P. Grishchuk, A. G. Doroshkevich, and V. M. Yudin, *Zh. Eksp. Teor. Fiz.* **69**, 1857 (1975) [*Sov. Phys. JETP* **42**, 943 (1976)].
- [27] A. Pontzen and A. Challinor, in preparation (2009).
- [28] J. D. Barrow, *Phys. Rev. D* **51**, 3113 (1995).
- [29] J. Wainwright, *Dynamical Systems in Cosmology* (Cambridge University Press, 1997).
- [30] G. F. R. Ellis and H. van Elst, *Cargèse lectures* (1998), arXiv:gr-qc/9812046
- [31] S. Hawking, *Mon. Not. R. Astron. Soc.* **142**, 129 (1969).
- [32] S. Seager, D. D. Sasselov, and D. Scott, *Astrophys. J. Lett.* **523**, L1 (1999).
- [33] T. R. Jaffe *et al.*, *Astrophys. J.* **643**, 616 (2006).
- [34] K. Land and J. Magueijo, *Mon. Not. R. Astron. Soc.* **367**, 1714 (2006).
- [35] M. Demiański and A. G. Doroshkevich, *Phys. Rev. D* **75**, 123517 (2007).
- [36] J. Wainwright, A. A. Coley, G. F. R. Ellis, and M. Hancock, *Classical and Quantum Gravity* **15**, 331 (1998).
- [37] J. A. Peacock, *Cosmological physics* (Cambridge University Press, Cambridge, UK, 1999).
- [38] D. H. King, *Phys. Rev. D* **44**, 2356 (1991).
- [39] J. A. Wolf, *C. R. Acad. Sci.*, **250**, 3443 (1960).
- [40] J. M. Bardeen, *Phys. Rev. D* **22**, 1882 (1980).
- [41] K. Rosquist and R. T. Jantzen, *Phys. Rep.* **166**, 89 (1988).
- [42] A. Coley and S. Hervik, *Classical and Quantum Gravity* **22**, 579 (2005); S. Hervik, R. van den Hoogen and A. Coley, *Classical and Quantum Gravity* **22**, 607 (2005).
- [43] A. G. Doroshkevich, V. N. Lukash, and I. D. Novikov, *Zh. Eksp. Teor. Fiz.* **64**, 1457 (1973) [*Sov. Phys. JETP* **37**, 739 (1973)].
- [44] This decomposition can be made in the non-linear case [42] and is essentially an example of the automorphism approach to Bianchi dynamics (e.g. [41] and references therein).
- [45] During matter domination,  $\eta|a_1| \ll 1$ ; if  $a_1 \ll 1$ , the approximation  $\kappa \simeq 1$  follows immediately whereas if  $a_1 \sim \mathcal{O}(1)$  one may nonetheless approximate  $\kappa \simeq 1$  in all physical results by a suitable redefinition of the integration constant  $A_0 \rightarrow A_0/(1 - ia_1)^{3/2}$  (determined by a Laurent expansion of  $\sigma$  and  $S$  in  $\eta \ll 1$ ); the situation is, as expected, physically indistinguishable from the flat VII<sub>0</sub> case ( $a_1 = 0$ ).
- [46] Claims that the anisotropic curvature causes the shear to diverge logarithmically towards the initial singularity, e.g. [28, 43], rely on time-averaging over multiple oscillation periods; this is meaningful only in models where  $\eta \gg 1$  at matter-radiation equality, demanding  $x \ll \sqrt{\Omega_R}/\Omega_M \sim 0.03$  for which case the linearisation (2) is inapplicable; see [27] for more details. Even with the logarithmic divergence the nucleosynthesis constraints are drastically weakened over power-law divergences [20, 22].
- [47] See PC07 eq. 23; in fact it is possible to show that the  $p_i$  remain constant because the geodesics describe the integral curves of the Killing fields, a situation which is also true of the flat Type I models but which can never be arranged for open models. This is true simply by enumeration of the Bianchi types, but can be seen to arise from the divergence of geodesics in hyperbolic spaces [39].